Send Orders for Reprints to reprints@benthamscience.ae

Current Alzheimer Research, 2016, *13*, 000-000

Early β-Amyloid-induced Synaptic Dysfunction is Counteracted by Estrogen in Organotypic Hippocampal Cultures

Sara Merlo[a], Simona Federica Spampinato[a], Francisco Capani[b] and Maria Angela Sortino[a,*]

[a]*Department of Biomedical and Biotechnological Sciences, Section of Pharmacology, University of Catania, Catania, Italy,* [b]*Facultad de Medicina, Instituto de Investigaciones Cardiológicas "Prof. Dr. Alberto C. Taquini" (ININCA), Universidad de Buenos Aires (CONICET) Buenos Aires, Argentina*

Please provide corresponding author(s) photograph

Abstract: In the present study we set up a model of slow progression of neuronal injury by exposing organotypic hippocampal cultures to a low concentration of Amyloid β (25-35) peptide (Aβ, 2 μM) to analyze the time-related effects of 17-β estradiol (17β-E2, 10 nM). Neuronal death occurs after 7 d and is prevented by addition of 17β-E2 24 h prior to, together with or 48 h after exposure to Aβ. This effect is mimicked by selective ERα agonist PPT (100 nM). Treatment with Aβ leads to early and transient (16-72 h) increase of pre- and post-synaptic proteins synaptophysin and PSD95, followed by a decrease coincident with neuronal death (7d), all prevented by 17β-E2. At 72 h of Aβ exposure, synaptic activity is increased, as by higher levels of glutamate and increased loading and unloading of FM 1-43-labeled synaptic vesicles. All these effects are also prevented by 17β-E2. These data point out beneficial effects of estrogen on early Aβ-induced synaptic disruption.

Keywords: 17β-estradiol, synaptic hyperactivity; synaptophysin; Alzheimer's Disease, estrogen receptor α.

1. INTRODUCTION

Estrogens play a central role in the development and homeostasis of the central nervous system (CNS), with neurotrophic, neurogenic and neurodifferentiative action. In addition, estrogens have well-documented neuroprotective effects in a number of pathological conditions such as Alzheimer's Disease (AD), autoimmune inflammation, traumatic injury and ischemia [1-6].

Estrogens activate specific receptors (ERs) on both neuronal and glial cells throughout the CNS. Two main subtypes have been identified, ERα and ERβ, each existing as alternative splice variants [7, 8]. At least another isoform (ERX), selectively localized at the cell membrane, is known to trigger signaling cascades at the cell surface [9]. All three known receptors as well as non-receptor mediated mechanisms have been differentially involved in estrogen neuroprotection [10].

AD is a progressive neurodegenerative disease affecting over 25 million worldwide. The key molecular factor in the etiology of the disease appears to be the misfolding and abnormal aggregation of an otherwise soluble neuronal protein, the β amyloid peptide. Aβ self-associates to form different size oligomers, which progressively assemble into fibrils that in turn form extracellular deposits in the brain [11, 12]. The oligomeric state has been shown to be the most neurotoxic, acting through several molecular mediators that trigger multiple effects on different pathways. Such complex patterns of synaptic dysfunction and network disorganization slowly lead to clinically relevant cognitive manifestations [13].

AD is among neurodegenerative pathologies for which evidence of a positive action of estrogen has been provided [14]. Despite strong support from *in vivo*, *in vitro* and epidemiological studies, the therapeutic potential of estrogens in AD is still controversial due to the observation that delayed estrogen exposure may result ineffective or even detrimental, highlighting the significance of the timeliness of exposure to estrogens in AD therapy [2, 15-17]. On these bases, we undertook this study to shed light on the mechanisms through which estrogens affect slow maturation of Aβ – induced neuronal damage in the hippocampus. To this purpose, we used organotypic hippocampal slice cultures (OHC), largely utilized in neurodegeneration, neuroprotection and neurorepair studies, that provide integrity of cytoarchitecture and connective organization of the tissue of origin and more closely resemble the functional characteristics of the hippocampal formation *in vivo* [18].

2. MATERIALS AND METHODS

2.1. Drugs

Aβ(25-35) (Bachem, Feinchemikalien AG, Bubendorf, Switzerland) was reconstituted in sterile deionized water at a concentration of 2 mM and stored in aliquots at -20°C.

Aβ(1-42) peptide (Innovagen, Lund, Sweden) was solubilized in DMSO as a 5 mM stock, then diluted to 100 μM in culture medium. For experiments, 100 μM Aβ(1-42) was aggregated into oligomers by overnight incubation at 4°C followed by a freeze-thaw cycle.

*Address correspondence to this author at the Department of Biomedical and Biotechnological Sciences, Section of Pharmacology, University of Catania, School of Medicine, Via S. Sofia 64, 95125 Catania, Italy;
E-mail: msortino@unict.it

1567-2050/16 $58.00+.00 © 2016 Bentham Science Publishers

17β-E2 (Sigma-Aldrich Co, Milan, Italy), 1,3,5-tris(4-hydroxyphenyl)-4-propyl-1H- 20 pyrazole and diarylpropionitrile (PPT and DPN; Tocris Cookson Ltd, North Point, UK) were dissolved in ethanol to a concentration of 10 mM. Subsequent dilutions were made in aqueous solution so that the amount of vehicle was always less than 0.01%.

2.2. Preparation of Rat Organotypic Hippocampal Slice Cultures

OHC obtained from P7 Sprague-Dawley rats were cultured with the interface method as previously described [19], with slight modifications. Briefly, each hippocampus was isolated and cut into 350 μm-thick transversal sections with a McIlwain tissue chopper. Intact slices were selected and incubated for 20 minutes at 4°C in Hank's Balanced Salt Solution (Invitrogen, Milan, Italy) supplemented with 0.5% glucose (Sigma) and 1.5% Fungizone (Invitrogen). Slices were then transferred onto Millicell-CM culture inserts (Millipore Merck KGaA Darmstadt, Germany; 4 slices/insert) placed on top of 1 ml of Eagle's minimal essential medium (MEM) containing 25% HBSS, 25% horse serum (HS), 1 mM glutamine, 1.5% Fungizone (all from Invitrogen) and 0.5% glucose (Sigma). For experiments in serum-free conditions, HS was substituted with an equivalent volume of MEM. Cultures were incubated at 37°C and 5% CO_2 in a humidified atmosphere and subjected to medium change twice a week. Slices were used for experiments after 14 days of maturation *in vitro*. All animal experimental procedures were carried out in accordance with the directives of the Italian and European Union regulations for the care and use of experimental animals (DL116/92) and were approved by the Italian Ministry of Health.

2.3. Assessment of Cell Death by Propidium Iodide Staining

The extent of cell death was determined by staining of slices with propidium iodide (PI), a fluorescent DNA intercalating agent able to penetrate only in cells with a disrupted membrane. Slices were incubated at 37°C with 2.5 μg/ml PI for 25 minutes and washed with PBS. Images of whole slices were captured with an epifluorescent microscope with a 5X objective (Zeiss) connected to a digital camera. Fluorescence intensity was determined with the aid of the image processing software "Image J" developed by NIH and in public domain.

2.4. Western Blot Analysis

Four to eight slices per condition were pooled and transferred into a 1.5 ml-tube containing RIPA-lysis buffer (Sigma) supplemented with a protease- and phosphatase-inhibitor cocktail mix (Sigma). Full lysis was obtained by sonication of the samples. Based on the marker of interest, 10 to 50 μg of protein extract were separated by SDS-PAGE and transferred to nitrocellulose membranes (Hybond ECL, Amersham Biosciences Europe GmbH, Milan, Italy) using a Transblot semidry transfer cell. Membranes were blocked in Odyssey blocking buffer (LI-COR Biotechnology GmbH, Bad Homburg, Germany) diluted 1:1 with PBS containing 0.1% Tween-20, and probed with the following antibodies: mouse anti-β-actin (1:1000; Sigma), mouse anti-α-tubulin (1:10000; Sigma), mouse anti-ERα (1:500; Millipore), rabbit anti-ERβ (1:200; Santa Cruz–Biotechnologies, Santa Cruz, CA, USA), mouse anti- SYP (1:10000; S. Cruz), rabbit anti-PSD-95 (1:1000; Cell Signaling Danvers, MA, USA), mouse anti-GFAP (1:10000; Cell Signaling), rabbit anti-Iba1 (1:700; Biocare Medical, Concord, CA, USA) and IRDye®680 or IRDye®800-conjugated secondary antibodies (LI-COR). Detection of specific bands was carried out using the Licor Odyssey® Infrared Imaging System (LI-COR). Band intensity was analyzed using the Image J software.

2.5. Immunofluorescent Staining

Slices were fixed by submersion in 4% paraformaldehyde at 4° overnight, followed by extensive washing in PBS. For immunostaining, each slice was detached from the insert membrane with the aid of a flexible plastic spatula and transferred into a 1.5 ml-tube containing PBS. Floating slices were blocked/permeabilized with 3% BSA in PBS containing 0.1% Triton-X100 for 2 h at room temperature (RT), then incubated with the primary antibody in 3% BSA in PBS containing 0.05% Triton-X100 for 24 h at 4°C and finally with fluorochrome-conjugated secondary antibodies for 2 h. Antibodies used were: mouse anti-ERα (1:500; Millipore), mouse anti-SYP (1:200; S. Cruz); mouse anti-GFAP (1:400; Cell Signaling), rabbit anti-Iba1 (1:700; Biocare), Alexa Fluor 488 anti-mouse (1:300; Invitrogen), Alexa Fluor 546 anti-mouse (1:300; Invitrogen). Digital images were captured with a Zeiss Observer.Z1 microscope equipped with the Apotome.2 acquisition system. SYP staining was quantified by determination of number and mean area of positive puncta with CellProfiler Software for automated biological image analysis [20]. Analysis was performed on 3 random fields of the CA1 area per slice on 63X magnification images, from at least 4-6 slices for each treatment condition. Slices from three different cultures were analyzed.

2.6. Glutamate Assay

Medium from OHC exposed to treatments was collected into aliquots and kept frozen until use. Levels of glutamate in each sample were measured with a commercial colorimetric Glutamate Assay Kit (Sigma), strictly following the manufacturer's instructions. Absorbance was measured at 450 nm with Varioskan™ Flash Multimode Reader.

2.7. FM 1-43 Dye Loading and Imaging

Experiments were carried out according to a previously published protocol [21], with slight modifications. OHC were washed in a modified Tyrode solution (TS; in mM: 150 NaCl, 4 KCl, 2 $MgCl_2$, 10 glucose, 10 HEPES, and 2 $CaCl_2$, pH 7.4), exposed to 10 μM FM 1-43 dye (Invitrogen) in the same buffer for 5 min to label membranes, then stimulated with high-potassium (90 mM KCl) TS (HKTS; containing equimolar substitution of KCl for NaCl) for 10 min to stimulate synaptic vesicle exocytosis. After HKTS removal, slices were subjected to a 15 min recovery in the presence of FM 1-43 (10 μM) to allow complete recycling of synaptic vesicles, then extensively washed with TS to remove excess dye. Finally, OHC were stimulated with HKTS for 15 min to allow complete unloading of dye-labeled vesicles. All steps were carried out in the presence of (2,3-dihydroxy-6-nitro-7-

sulfamoyl-benzo[f]quinoxaline-2,3-dione (NBQX, 10 μM) to prevent recurrent activity during stimulation. Images were captured at the end of wash (coinciding with complete loading) and at the end of unloading using a Zeiss Observer. Z1 microscope connected to a digital camera. Quantitative analysis of fluorescence intensity after loading and unloading in the CA1 area was performed on 10X magnification images of the same field with CellProfiler Software for automated biological image analysis [20]. The bleach/spontaneous release rate was negligible. At least 4-8 slices for each treatment condition and from three different cultures were analyzed.

2.8. Statistical Analysis

All experiments were run at least in triplicate and carried out 4–6 times. Analysis was performed by Student's t-test or one-way ANOVA followed by Newman–Keuls test for significance, with GraphPad Prism Software for Windows (GraphPad Software, San Diego, California USA).

3. RESULTS

The expression of estrogen receptors (ERs) in OHC was evaluated by Western blot analysis (Fig. **1a,c**). As shown, both ERα and ERβ subtypes are expressed in basal conditions, the former being present as two different molecular weight isoforms of 66 kDa and 46 kDa (Fig **1a,c**). Treatment with 10 μM Aβ(25-35) for 24 h induces a significant increase of both the 66 kDa (153% ± 9 vs. control) and the 46 kDa (119% ± 4 vs. control) isoforms of ERα but has no effect on ERβ expression (Fig. **1a**). Immunostaining of ERα in the same conditions appears to confirm Aβ-induced up-regulation (Fig. **1b**). Similarly, exposure to 2 μM Aβ(25-35) for 72 h increases expression of both the 66 kDa (131% ± 5 vs. control) and 46 kDa (145% ± 6 vs. control) isoforms without modifying ERβ expression (Fig. **1c**). In these conditions ERα immunostaining is widely distributed and apparently localized to more morphologically reactive cells following Aβ treatment (Fig. **1d**).

Effects of 17β-E2 on neuronal viability following a toxic stimulus were tested in OHC exposed to different concentrations of Aβ(25-35). Exposure to 10 μM of Aβ(25-35) leads to extensive neuronal death already after 24 h, as assessed by PI incorporation assay (Fig. **2a,b**). In these conditions, 10 nM 17β-E2 completely prevents neuronal death both when added 24 h prior to or together with Aβ treatment (Fig. **2a,b**). Use of a lower concentration of Aβ(25-35), i.e. 2 μM, allows chronic exposure to the peptide before reaching neuronal death, as evaluated by PI incorporation assay. At 16, 48 and 72 h no PI incorporation is present (not shown) while neuronal death appears after a 7 d treatment with 2 μM Aβ(25-35) (Fig. **2c,d**). In these conditions 10 nM 17β-E2, added together with Aβ(25-35), is once again totally protective (Fig. **2c,d**). In contrast, exposure to 500 nM aggregated Aβ(1-42) oligomers does not induce neuronal death up to 14 days, as assessed by PI staining, (not shown). When OHC are exposed to selective ERα and ERβ agonists, PPT (100 nM) and DPN (1 nM) respectively, different responses appear. In fact, PPT mimics the neuroprotective effect of 17β-E2 against Aβ(25-35) (2 μM for 7 d), while DPN only shows a partial, non-statistically significant reduction of PI incorporation (Fig. **2c,d**).

In order to assess whether alteration of synaptic protein function is a critical event in Aβ-induced neuronal death, time-course analysis of synaptic protein expression was carried out, by Western blot, during exposure to 2 uM Aβ(25-35) in the presence of 10 nM 17β-E2. The pre-synaptic marker SYP and post-synaptic marker PSD-95 were analyzed at 16 h, 72 h and 7 days of treatment. As shown in Fig. **3**, both SYP and PSD-95 show a similar profile of expression, with an early increase, compared to control, at 16 h (Fig. **3a**) or 72 h (Fig. **3b**) of treatment, and a decrease at 7 days (Fig. **3c**), coinciding with neuronal death. Both these effects yield statistically significant difference from control. 17β-E2 is able to contrast Aβ(25-35)-induced synaptic protein variations at all time-points, bringing protein levels back to respective control conditions (Fig. **3a,b** and **c**). Similar changes in synaptic protein expression were observed when OHC were exposed to 500 nM aggregated Aβ(1-42) oligomers for 7 d, a time-point when cell death is not detectable. Western blot analysis reveals a significant increase of both SYP and PSD95 in OHC exposed to Aβ(1-42), compared to control, an effect that is once again reverted by 10 nM 17β-E2 exposure (Fig. **3d**). In our conditions, treatment with 10 nM 17β-E2 does not *per se* modify synaptic protein expression (data not shown).

Immunocytochemical analysis of SYP expression in OHC shows a punctuate staining (Fig. **4a**). Quantitative evaluations of the number and mean area of SYP-positive puncta in the CA1 area show a significant increase in both the number (140 % ± 10.9 vs. control; Fig. **4b**) and mean area (133% ± 9 vs. control; Fig. **4c**) of puncta following 72 h of exposure to 2 μM Aβ(25-35), compared to untreated control. When 10 nM E2 is added together with Aβ, such effects on synaptic vesicle organization are prevented (vesicle number and mean area = 106% ± 8 and 107.6% ± 6.9 vs. control, respectively).

Effects of 17β-E2 on astrocytic (GFAP) and microglial (Iba1) markers upon Aβ(25-35) exposure were analyzed by Western blot and immunostaining (Fig. **5**). A significant increase of both GFAP (Fig. **5a**) and Iba1 (Fig. **5b**) is induced by a 72 h exposure to 2 μM Aβ, compared to control conditions. Ten nM 17β-E2 has no effect on Aβ-induced GFAP increase (Fig. **5a**) while it prevents Iba1 up-regulation (Fig. **5b**). Corresponding immunostaining of GFAP and Iba1 are shown in Fig. **5c** and **d**, respectively.

Released glutamate (Glu) levels were measured in the culture medium using a commercial Glutamate Assay Kit. Glu levels are unchanged after short-term Aβ exposure (2 μM Aβ(25-35) for 30 min or 6 h; not shown), whereas they are significantly increased, compared to control, after 72 h of Aβ treatment (Fig. **6a**). Such effect is prevented by 10 nM 17β-E2 (Fig. **6a**). At this time point, synaptic vesicle loading and unloading were evaluated by labeling with the FM 1-43 dye. A slight increase of vesicle loading (that however does not yield significance) is observed following exposure to 2 μM Aβ(25-35), as by the higher fluorescence intensity at the end of loading step, compared to control (Fig. **6b,d**). Of note, treatment with 10 nM 17β-E2 not only prevents this increase, but significantly reduces also basal vesicle loading (Fig. **6b,d**). Vesicle unloading is expressed as percent residual fluorescence vs. respective fluorescence at time 0 (end of

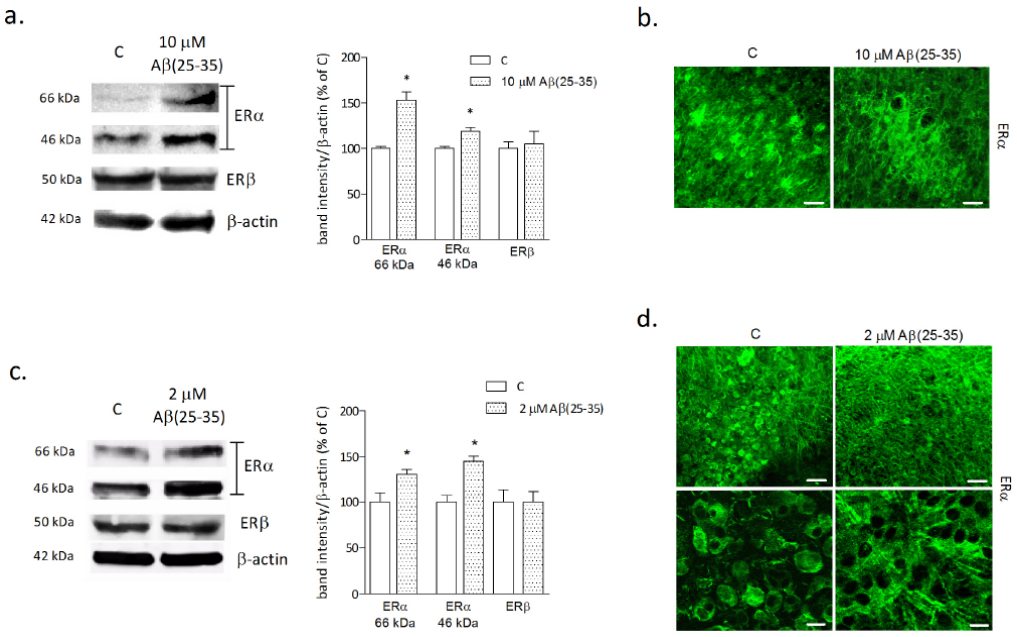

Fig. (1). ERs expression in OHC. In a, Western blot analysis of ERα and ERβ in OHC exposed to 10 μM Aβ(25-35) for 24 h, normalized to β-actin. In b, representative image of immunostaining of ERα in the same conditions. Scale bar is 30 μm. In c**, Western blot analysis of ERα and ERβ in OHC exposed to 2 μM Aβ(25-35) for 72 h, normalized to β-actin.** In d, representative 20X (top panels) and 63X (bottom panels) magnification images of immunostaining for ERα in control and treatment conditions (2 μM Aβ(25-35) for 72 h). Scale bars are 40 μm for 20X captions and 10 μm for 63X captions. Representative blots are shown. Bars are mean ± SEM of at least three independent experiments. *p<0.05 vs. respective control by Student's t-test for significance.

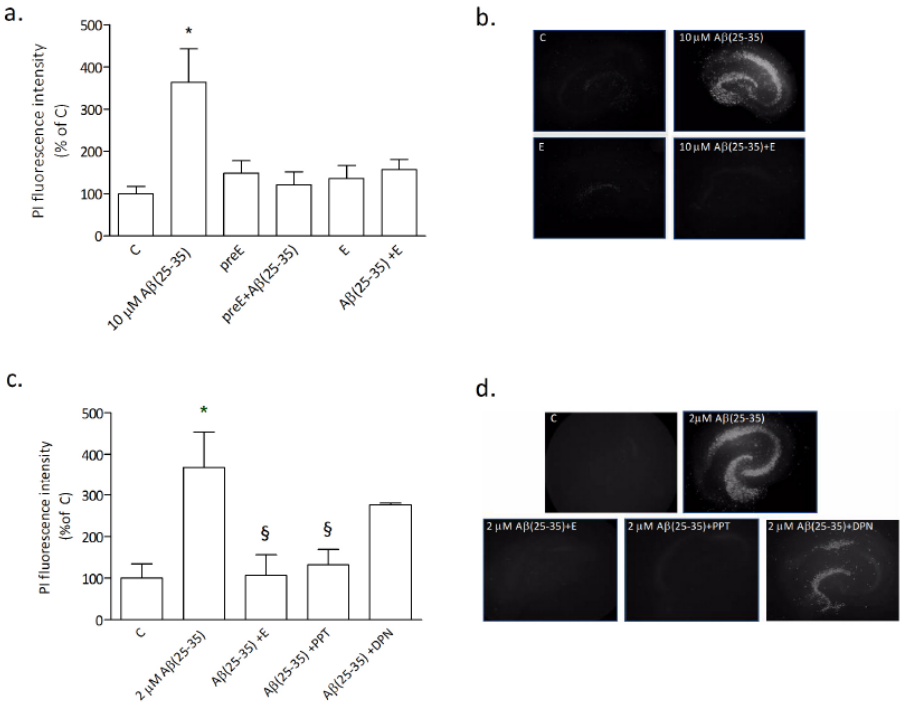

Fig. (2). Estrogen's effects on Aβ toxicity in OHC. Cell death was evaluated as mean fluorescence intensity of incorporated PI in OHC exposed to different treatments. In a, values for PI incorporation in OHC treated with Aβ(25-35) alone (2 μM for 24 h) or in combination with 10 nM 17β-E2, added 24 h prior to Aβ and maintained during the following 24 h [preE + Aβ(25-35)], or together with Aβ (Aβ(25-35) + E) for 24 h. Representative images of PI incorporation in these conditions, at 5X magnification, are reported in b. In c, PI incorporation following exposure to 2 μM Aβ(25-35) alone for 7 d or in co-treatment with 10 nM 17β-E2, 100 nM ERα selective agonist PPT, or 1 nM ERβ selective agonist DPN. **Corresponding captures of PI incorporation are reported in d (5X magnification).** Bars are mean ± SEM of at least three independent experiments. *p<0.05 vs. other groups and § p<0.05 vs. 2 μM Aβ(25-35) alone by one-way-ANOVA followed by Newman-Keuls test for significance.

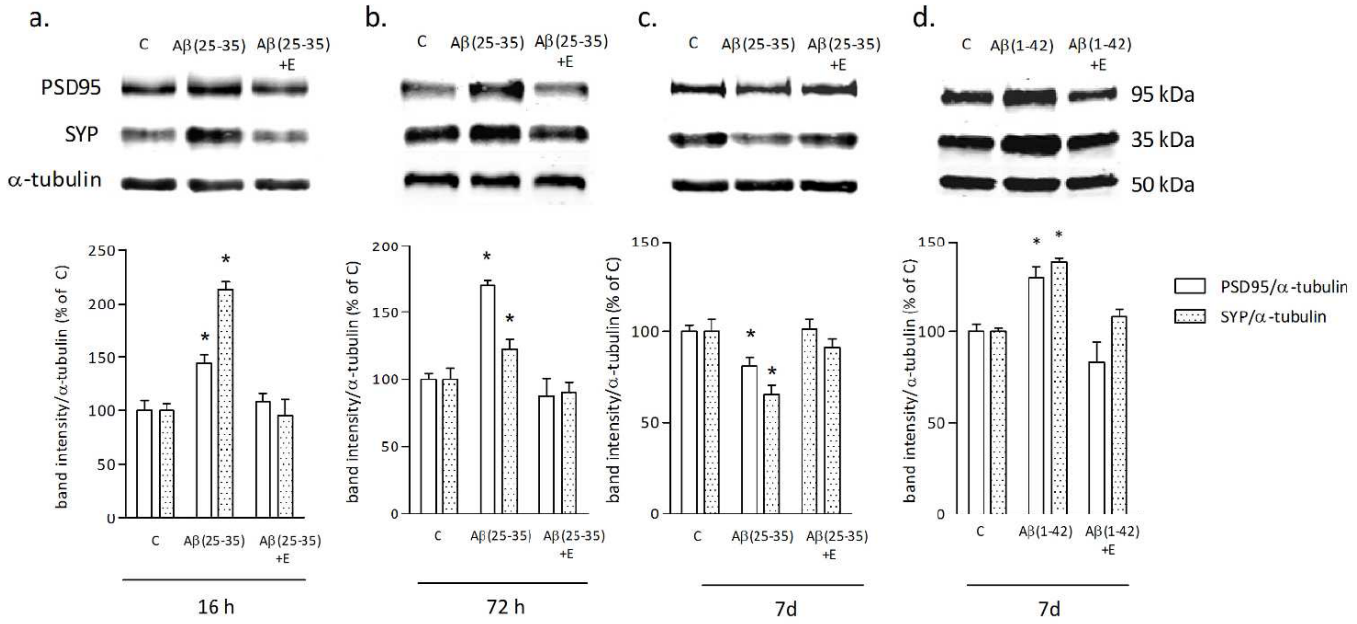

Fig. (3). Time course analysis of estrogen effects on synaptic protein expression in Aβ-challenged OHC. Expression of pre- (SYP) and post-synaptic (PSD95) proteins as evaluated by Western blot at 16 h (a), 72 h (b) and 7 d (c) of exposure to 2 μM Aβ(25-35) alone or in combination with 10 nM 17β-E2 (E). In d, Western blot of SYP and PSD95 in OHC treated for 7 d with 0.5 μM Aβ(1-42) alone or in combination with 10 nM 17β-E2. In all blots α-tubulin was used for normalization. Representative blots are shown. Bars are mean ± SEM of at least three independent experiments. *p<0.05 vs. other respective groups, by one-way-ANOVA followed by Newman-Keuls test for significance.

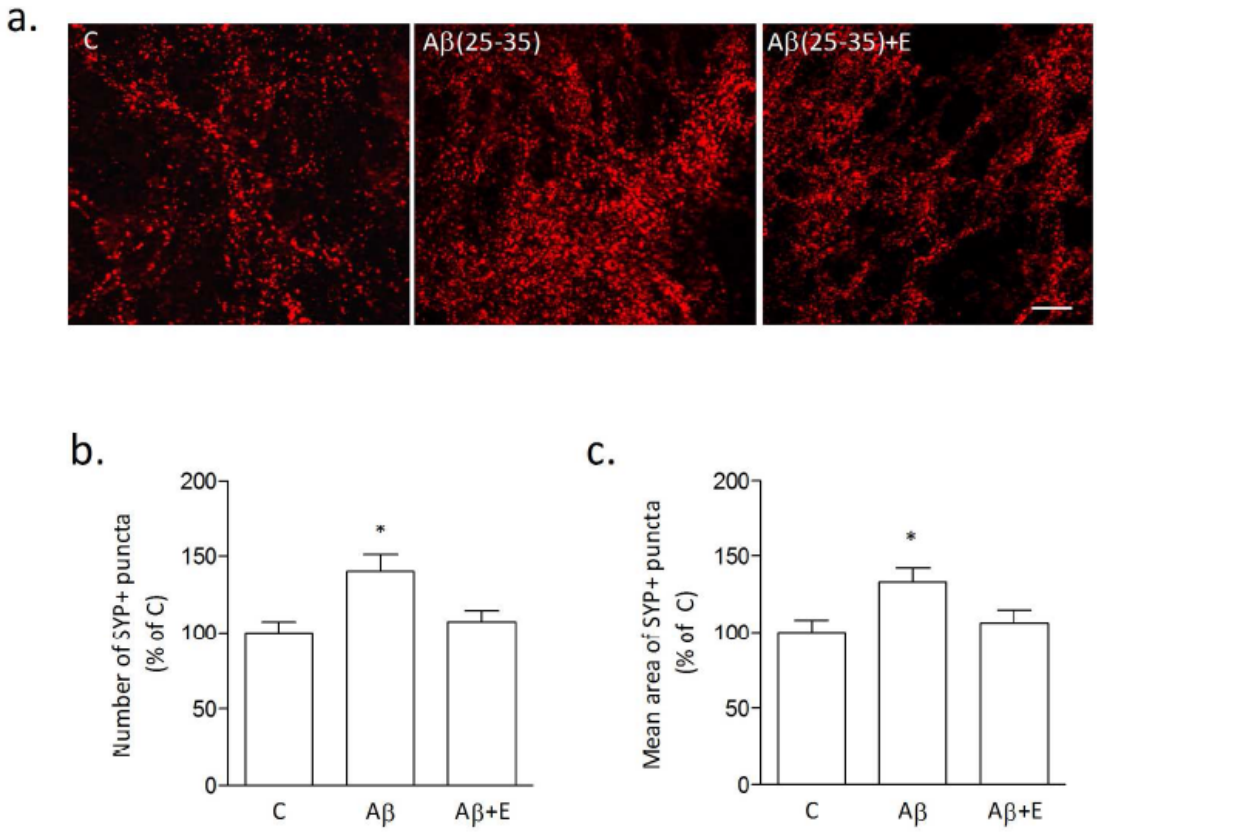

Fig. (4). Estrogen's effects on re-organization of synaptic structure in Aβ-challenged OHC. In a, representative image of a 63X magnification field of OHC CA1 area, immunostained for SYP (scale bar is 10 μm). Number (b) and size (c) of SYP+ puncta in OHC exposed to Aβ(25-35) alone (2 μM for 72 h) or with 10 nM 17β-E2 (E) are reported, as by automatic software determination. Bars are mean ± SEM of at least three independent experiments. *p<0.05 vs. other groups by one-way-ANOVA followed by Newman-Keuls test for significance.

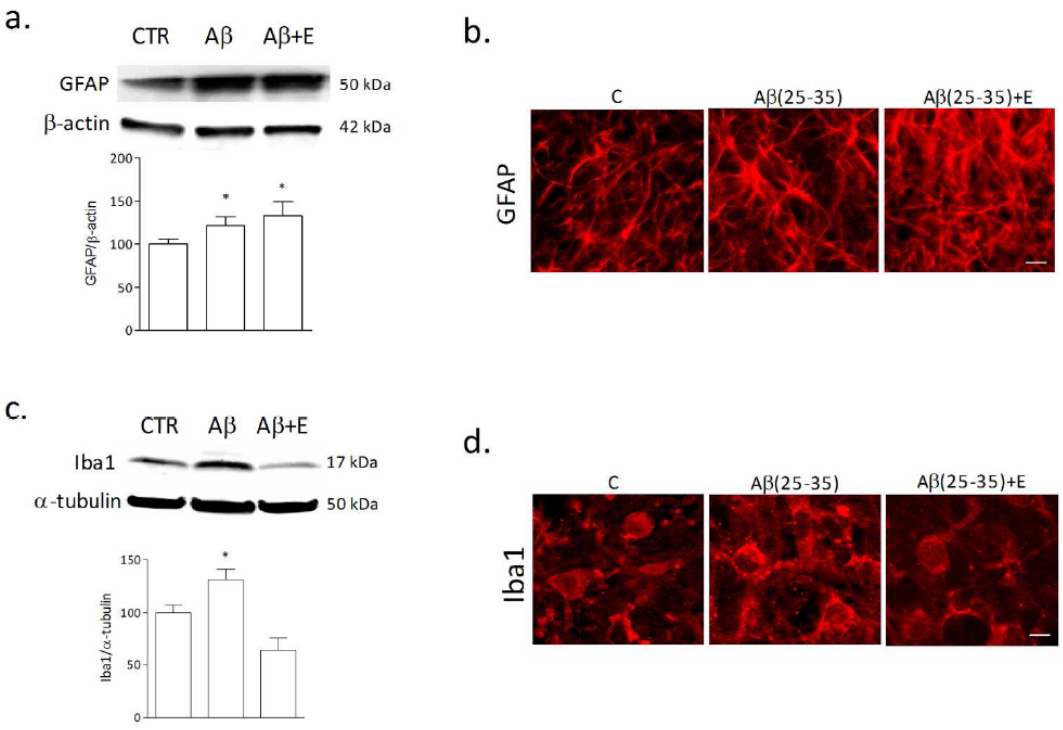

Fig. (5). Estrogen's effects on glial cells in Aβ-challenged OHC. Western blot analysis of GFAP (a) and Iba1 (b) levels in OHC treated for 72 h with 2 μM Aβ(25-35) alone or in the presence of 10 nM 17β-E2 (E). β-actin and α-tubulin were used for normalization of GFAP and Iba1, respectively. In c and d, representative images of immunostaining for GFAP (c; 40X magnification, scale bar 10 μm) and Iba1 (d; 63X magnification, scale bar 5 μm) in the same conditions. Representative blots are shown. Bars are mean ± SEM of at least three independent experiments. *p<0.05 vs. other groups by one-way-ANOVA followed by Newman-Keuls test for significance.

loading), set as 100%. Exposure to 2 μM Aβ(25-35) induces a significant decrease of residual fluorescence, compared to control, indicative of enhanced vesicle unloading (Fig. **6c,d**). This effect is prevented by 10 nM 17β-E2 (Fig. **6c,d**). Fig **6d** reports representative images of loading (L) and unloading (U) steps for each condition.

Experiments were then carried out to evaluate if addition of 17β-E2 to OHC previously exposed to Aβ could still be protective. OHC were exposed to 2 μM Aβ(25-35) for 48 h, prior to addition of 10 nM 17β-E2 for further 5 d, still in the presence of Aβ. Analysis of cell death by PI staining in these conditions reveals that delayed exposure to 17β-E2 or the selective ERα agonist PPT maintains the ability to partially rescue neurons from Aβ-induced death, compared to untreated control conditions (Fig. **7a**). Evaluation of SYP and PSD95 levels in OHC subjected to a 48 h-pre-treatment with 2 μM Aβ(25-35) alone, followed by further 24 h exposure to Aβ in combination with 10 nM 17β-E2 or 100 nM PPT, was carried out by Western blot. In these conditions, neither 17β-E2 nor PPT prevent Aβ-induced up-regulation of SYP and PSD95 compared to control (Fig. **7b**).

4. DISCUSSION

The activity of estrogen as a neuroprotective agent in neurodegenerative conditions, such as AD, has been well established over the past years [2, 22-24]. However, a number of reports suggesting a harmful action of the hormone still need to be taken into account [24-28] in order to fully appraise the potential of hormone replacement therapies. Timing of estrogen exposure in particular seems to be crucial to determine alternatively favorable or harmful effects [2, 16, 29, 30]. Moved by these considerations, we here aimed to dissect the events triggered in response to chronic exposure to a toxic stimulus and the mechanisms through which estrogens rescue neurons from death in such conditions. We thus set up an *in vitro* model using OHC exposed to a low concentration of the β-amyloid peptide. Aβ is the key player in AD onset and its neurotoxicity has been linked to synaptic dysfunction and network disorganization, that underlie progressive cognitive decline [13]. In our model, neuronal damage matures slowly, leading to cell death in a reasonably wide time span. This allows analysis of early events taking place at a time of particular sensitivity to hormonal exposure. Preliminary experiments were carried out with either the active Aβ fragment 25-35 or the full length aggregated Aβ(1-42) and yielded comparable results, allowing further experiments to be carried out with Aβ(25-35). Consistent with our results, the equivalent effects of the two peptides has been shown in a comparative toxicity study using OHC [31]. Our interest was focused on the hippocampal formation for it is one of the first targets of Aβ toxicity in the AD brain [32] and the OHC model was chosen because of its unique preservation of original hippocampal cytoarchitecture and neuronal circuitry [18, 33-35].

Based on the notion that synaptic dysfunction is one of the first steps on the road that ultimately leads to neuronal degeneration, we analyzed expression of two key pre- and post-synaptic markers, SYP and PSD95. Time course analysis reveals, upon Aβ exposure, a rapid and long-lasting in-

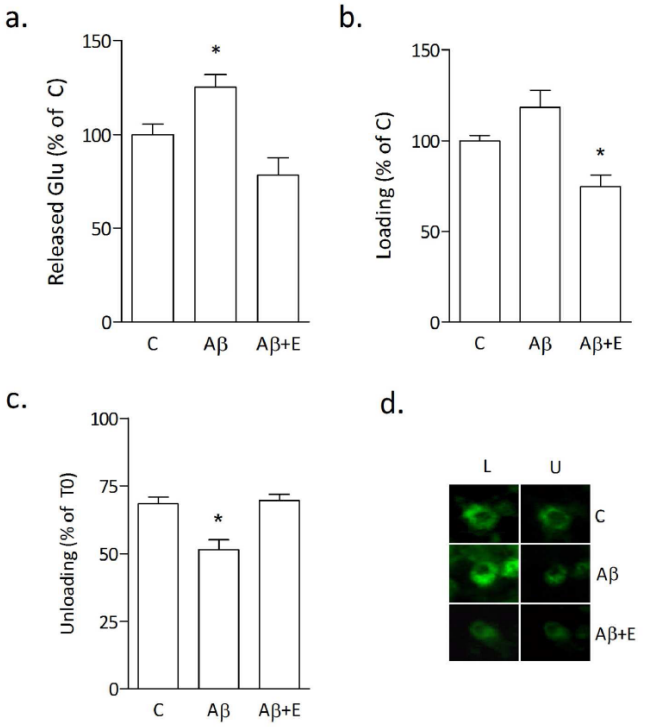

Fig. (6). Estrogen's effects on modified synaptic activity in Aβ-challenged OHC. In a, levels of released Glu assayed in culture medium with a specific commercial kit. Medium was collected from OHC exposed to Aβ(25-35) (2 μM for 72 h) alone or in the presence of 10 nM 17β-E2 (E; a). Loading (b) and unloading (c) of synaptic vesicles as determined by FM 1-43 dye fluorescence measurements in OHC treated with 2 μM Aβ(25-35) alone or with 10 nM 17β-E2 for 72 h. Loading fluorescence is reported as percent variation of treatment vs. control conditions (b), while unloading measurements are reported as variation vs. respective time zero (c). In d, representative images of cells at the end of loading (L) and unloading (U) steps for each treatment condition. Bars are mean ± SEM of at least three independent experiments. *p<0.05 vs. other groups by one-way-ANOVA followed by Newman-Keuls test for significance.

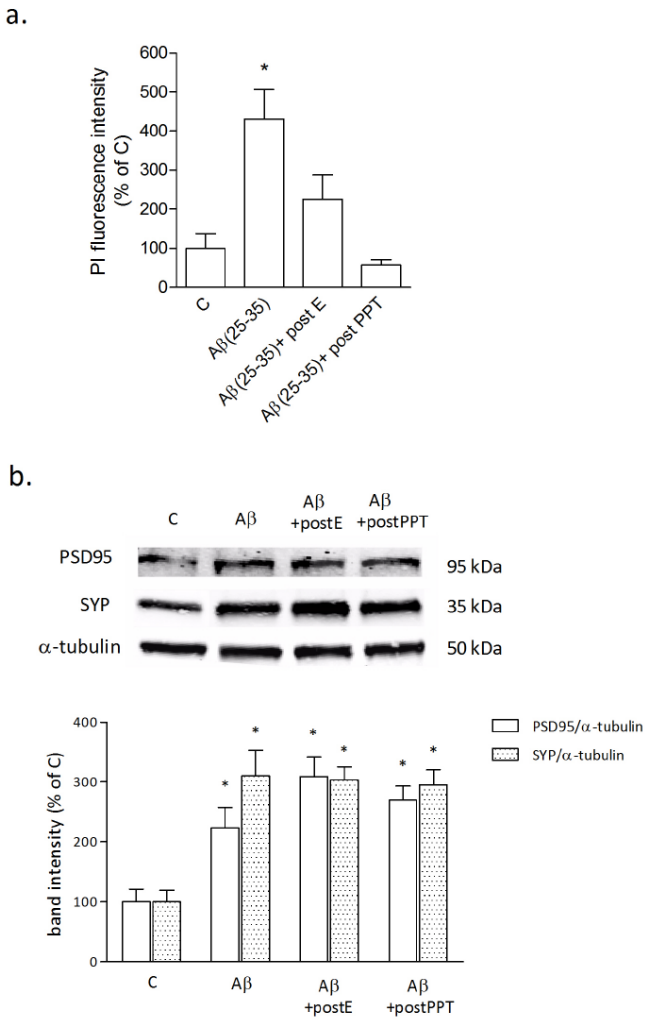

Fig. (7). Effects of delayed addition of 17β-E2 to OHC pre-exposed to Aβ. OHC were exposed to 2 μM Aβ(25-35) alone for either 72 h, or for 48 h followed by co-incubation with 10 nM 17β-E2 (Aβ(25-35)+post E) or 100 nM PPT (Aβ(25-35)+post PPT) for further 24 h. PI incorporation (a) and **Western blot analysis of PSD95 and SYP levels (b) in these conditions are shown**. Western blot bands were normalized to α-tubulin. Representative blots are shown. Bars are mean ± SEM of at least three independent experiments. *p<0.05 vs. control by one-way-ANOVA followed by Newman-Keuls test for significance.

crease of both SYP and PSD95 proteins preceding the sharp decrease coincident with neuronal loss. Such event may be interpreted as an attempted neuronal response to synaptic failure through increase of synaptic components. The effects of Aβ toxicity on synaptic function have been widely studied, yielding contrasting results based on the brain area examined and the severity of disease [36]. What has emerged, in full agreement with our own results, is that while synaptic loss is the final outcome, a transitional increase of at least some pre- and post-synaptic proteins, namely synaptophysin [37], drebrin [38], alpha-synuclein and PSD95 [39, 40], is likely to occur at a very early stage of disease. Such synaptic alterations, at least in the neocortex, precede the emergence of cognitive impairment [36]. This topic is currently highly debated, for the real significance of this transient neuronal hyperactivity in the pre-symptomatic stages of AD has not yet been identified, as extensively discussed [41]. In order to establish whether the altered synaptic composition we report is linked to altered vesicle/neurotransmitter release, we tested both glutamate levels and loading/unloading capabilities of OHC. Our data show a significant increase of glutamate first detectable in the culture medium after 72 h of stimulation with Aβ, paired to a significant increase of both synaptic vesicle exocytosis and recycling at the same time point. Accordingly, Aβ has been reported to increase glutamate levels, an event that triggers a variety of responses unfavorable to neuronal survival [42] and also impacts synaptophysin function leading to increased exocytosis [43]. An effect of Aβ on vesicle loading and unloading in pure hippocampal neuronal cultures has already been reported [44, 45], but due to the cellular model used and probably to the chosen time, a reduction of vesicle trafficking was observed in those studies. The correlation we here show between abnormalities in synaptic protein expression and glutamatergic transmission finds support in the literature. The rise of syn-

aptic markers has been in fact shown to be paralleled by increase of glutamatergic bouton density in patients with mild cognitive impairment [46] and paradoxical increases in hippocampal activation during prodromal AD [47], confirming our present observation that both events occur at early phases of neurodegeneration.

Analysis of estrogen receptor expression in our model confirms the presence of both ERα and ERβ. Expression of both ERs has been reported in different regions of the hippocampus, in pyramidal neurons as well as in interneurons, with both nuclear and extra-nuclear localization [48-50]. We report that Aβ exposure is able to modify expression of ERα, leading to its marked up-regulation, whereas no effect is evident on ERβ expression. Consistent with our results, previous reports have shown the up-regulation of ERα in different areas of the AD brain, such as the nucleus basalis of Meynert [51], the vertical limb of the diagonal band of Broca [52] and the hippocampus [53]. In addition, our present data show that use of the selective agonists for the two receptor subtypes distinguishes ERα as the main mediator of estrogen protective effects against Aβ-induced neuronal death. ERα activation has been shown to trigger a variety of protective mechanisms against Aβ toxicity, both directly in neurons [30, 54-56] and indirectly on the astroglial component of the CNS [57]. Such mechanisms include inhibition of Aβ-induced apoptotic pathways and induction of protective cell signaling [56, 58], as well as direct action on Aβ levels by increased degradation [59, 60] and decreased synthesis [61]. Furthermore, ERα directly interacts with membrane components such as glutamate receptors [30], the voltage-dependent anion channel (VDAC) [62] or insulin growth factor receptor [63], all involved at some level in cell response to Aβ. We now report that the synaptic derangement caused by Aβ in our experiments is completely prevented when 17-βE2 is added at physiological concentrations. Interestingly, neuroprotection by estrogen relies also in additional effects on other cell types. The increased microglia activation induced by low concentrations of Aβ is in fact counteracted by 17β-E2 treatment, suggesting an important action of estrogen in preventing the active role of microglia in Aβ toxicity [64, 65]. In contrast the slightly enhanced GFAP expression induced by Aβ is maintained in the presence of 17β-E2. This may result in a favorable effect as reactive astrocytes are known to mediate neuroprotection by estrogen [57, 66].

Notably, even when added up to 48 h after previous exposure to Aβ, estrogen is still neuroprotective. The lack of effect on the synaptic alterations that have already progressed at this time, suggests involvement of alternative mechanisms. At any rate, the delay between changes of synaptic protein expression and glutamate increase (16 h vs. 72 h) are indicative of sequential modification of the synapse and alteration of neurotransmission, allowing to speculate the intriguing possibility that estrogens exert a dual action. This implies distinct effects on synaptic structure and on glutamate release/excitotoxicity. Overall these observations appear particularly promising for they broaden the time window to be considered for successful therapeutic intervention with estrogens. Hence, in contrast to what generally thought, even during progression of neurodegeneration, at early time points, the possibility still exists for estrogen to exert a neuroprotective effect.

CONFLICT OF INTEREST

The author(s) confirm that this article content has no conflict of interest.

ACKNOWLEDGEMENTS

This work was supported by institutional funds (21040108) to MA Sortino.

REFERENCES

[1] Brinton RD. Cellular and molecular mechanisms of estrogen regulation of memory function and neuroprotection against Alzheimer's disease: recent insights and remaining challenges. Learn Mem 8(3): 121-33.(2001).

[2] Correia SC, Santos RX, Cardoso S, Carvalho C, Santos MS, Oliveira CR, *et al.* Effects of estrogen in the brain: is it a neuroprotective agent in Alzheimer's disease? Curr Aging Sci 3(2): 113-26.(2010).

[3] Spence RD, Voskuhl RR. Neuroprotective effects of estrogens and androgens in CNS inflammation and neurodegeneration. Front Neuroendocrinol 33(1): 105-15.(2012).

[4] Inagaki T, Etgen AM. Neuroprotective action of acute estrogens: animal models of brain ischemia and clinical implications. Steroids 78(6): 597-606 (2013).

[5] McCarthy MM. What can development teach us about menopause? Brain Res 1379: 109-18 (2011).

[6] Chakrabarti M, Haque A, Banik NL, Nagarkatti P, Nagarkatti M, Ray SK. Estrogen receptor agonists for attenuation of neuroinflammation and neurodegeneration. Brain Res Bull 109C: 22-31 (2014).

[7] Taylor SE, Martin-Hirsch PL, Martin FL. Oestrogen receptor splice variants in the pathogenesis of disease. Cancer Lett 288(2): 133-48 (2010).

[8] Heldring N, Pike A, Andersson S, Matthews J, Cheng G, Hartman J, *et al.* Estrogen receptors: how do they signal and what are their targets. Physiol Rev 87(3): 905-31 (2007).

[9] Toran-Allerand CD, Guan X, MacLusky NJ, Horvath TL, Diano S, Singh M, *et al.* ER-X: a novel, plasma membrane-associated, putative estrogen receptor that is regulated during development and after ischemic brain injury. J Neurosci 22(19): 8391-401 (2002).

[10] Simpkins JW, Singh M, Brock C, Etgen AM. Neuroprotection and estrogen receptors. Neuroendocrinology 96(2): 119-30 (2012).

[11] Walsh DM, Teplow DB. Alzheimer's disease and the amyloid beta-protein. Prog Mol Biol Transl Sci 107: 101-24 (2012).

[12] Selkoe DJ. Alzheimer's disease. Cold Spring Harb Perspect Biol 3(7): (2011).

[13] Mucke L, Selkoe DJ. Neurotoxicity of amyloid beta-protein: synaptic and network dysfunction. Cold Spring Harb Perspect Med 2(7): a006338 (2012).

[14] Simpkins JW, Perez E, Wang X, Yang S, Wen Y, Singh M. The Potential for Estrogens in Preventing Alzheimer's Disease. Ther Adv Neurol Disord 2(1): 31-49 (2009).

[15] Jamshed N, Ozair FF, Aggarwal P, Ekka M. Alzheimer disease in post-menopausal women: Intervene in the critical window period. J Midlife Health 5(1): 38-40 (2014).

[16] Daniel JM. Estrogens, estrogen receptors, and female cognitive aging: the impact of timing. Horm Behav 63(2): 231-7 (2013).

[17] Luine VN. Estradiol and cognitive function: Past, present and future. Horm Behav 66(4): 602-18 (2014).

[18] Noraberg J, Poulsen FR, Blaabjerg M, Kristensen BW, Bonde C, Montero M, *et al.* Organotypic hippocampal slice cultures for studies of brain damage, neuroprotection and neurorepair. Curr Drug Targets CNS Neurol Disord 4(4): 435-52 (2005).

[19] Gerace E, Landucci E, Scartabelli T, Moroni F, Pellegrini-Giampietro DE. Rat hippocampal slice culture models for the evaluation of neuroprotective agents. Methods Mol Biol 846: 343-54 (2012).

[20] Lamprecht MR, Sabatini DM, Carpenter AE. CellProfiler: free, versatile software for automated biological image analysis. Biotechniques 42(1): 71-5 (2007).
[21] Gaffield MA, Betz WJ. Imaging synaptic vesicle exocytosis and endocytosis with FM dyes. Nat Protoc 1(6): 2916-21 (2006).
[22] Dhandapani KM, Brann DW. Protective effects of estrogen and selective estrogen receptor modulators in the brain. Biol Reprod 67(5): 1379-85 (2002).
[23] Simpkins JW, Singh M. More than a decade of estrogen neuroprotection. Alzheimers Dement 4(1 Suppl 1): S131-6 (2008).
[24] Sherwin BB. Estrogen and cognitive functioning in women: lessons we have learned. Behav Neurosci 126(1): 123-7 (2012).
[25] Rapp SR, Espeland MA, Shumaker SA, Henderson VW, Brunner RL, Manson JE, *et al.* Effect of estrogen plus progestin on global cognitive function in postmenopausal women: the Women's Health Initiative Memory Study: a randomized controlled trial. JAMA 289(20): 2663-72 (2003).
[26] Shumaker SA, Legault C, Kuller L, Rapp SR, Thal L, Lane DS, *et al.* Conjugated equine estrogens and incidence of probable dementia and mild cognitive impairment in postmenopausal women: Women's Health Initiative Memory Study. JAMA 291(24): 2947-58 (2004).
[27] Craig MC, Maki PM, Murphy DG. The Women's Health Initiative Memory Study: findings and implications for treatment. Lancet Neurol 4(3): 190-4 (2005).
[28] Maki PM, Henderson VW. Hormone therapy, dementia, and cognition: the Women's Health Initiative 10 years on. Climacteric 15(3): 256-62 (2012).
[29] Spampinato SF, Merlo S, Molinaro G, Battaglia G, Bruno V, Nicoletti F, *et al.* Dual effect of 17beta-estradiol on NMDA-induced neuronal death: involvement of metabotropic glutamate receptor 1. Endocrinology 153(12): 5940-8 (2012).
[30] Spampinato SF, Molinaro G, Merlo S, Iacovelli L, Caraci F, Battaglia G, *et al.* Estrogen receptors and type 1 metabotropic glutamate receptors are interdependent in protecting cortical neurons against beta-amyloid toxicity. Mol Pharmacol 81(1): 12-20 (2012).
[31] Frozza RL, Horn AP, Hoppe JB, Simao F, Gerhardt D, Comiran RA, *et al.* A comparative study of beta-amyloid peptides Abeta1-42 and Abeta25-35 toxicity in organotypic hippocampal slice cultures. Neurochem Res 34(2): 295-303 (2009).
[32] Moodley KK, Chan D. The hippocampus in neurodegenerative disease. Front Neurol Neurosci 34: 95-108.(2014).
[33] Bahr BA. Long-term hippocampal slices: a model system for investigating synaptic mechanisms and pathologic processes. J Neurosci Res 42(3): 294-305 (1995).
[34] Gahwiler BH, Capogna M, Debanne D, McKinney RA, Thompson SM. Organotypic slice cultures: a technique has come of age. Trends Neurosci 20(10): 471-7 (1997).
[35] Holopainen IE. Organotypic hippocampal slice cultures: a model system to study basic cellular and molecular mechanisms of neuronal cell death, neuroprotection, and synaptic plasticity. Neurochem Res 30(12): 1521-8 (2005).
[36] Arendt T. Synaptic degeneration in Alzheimer's disease. Acta Neuropathol 118(1): 167-79 (2009).
[37] Mukaetova-Ladinska EB, Garcia-Siera F, Hurt J, Gertz HJ, Xuereb JH, Hills R, *et al.* Staging of cytoskeletal and beta-amyloid changes in human isocortex reveals biphasic synaptic protein response during progression of Alzheimer's disease. Am J Pathol 157(2): 623-36 (2000).
[38] Counts SE, Nadeem M, Lad SP, Wuu J, Mufson EJ. Differential expression of synaptic proteins in the frontal and temporal cortex of elderly subjects with mild cognitive impairment. J Neuropathol Exp Neurol 65(6): 592-601 (2006).
[39] Leuba G, Savioz A, Vernay A, Carnal B, Kraftsik R, Tardif E, *et al.* Differential changes in synaptic proteins in the Alzheimer frontal cortex with marked increase in PSD-95 postsynaptic protein. J Alzheimers Dis 15(1): 139-51 (2008).
[40] Gong Y, Lippa CF, Zhu J, Lin Q, Rosso AL. Disruption of glutamate receptors at Shank-postsynaptic platform in Alzheimer's disease. Brain Res 1292: 191-8 (2009).
[41] Stargardt A, Swaab DF, Bossers K. The storm before the quiet: neuronal hyperactivity and Abeta in the presymptomatic stages of Alzheimer's disease. Neurobiol Aging 36(1): 1-11 (2015).
[42] Varga E, Juhasz G, Bozso Z, Penke B, Fulop L, Szegedi V. Amyloid-beta1-42 Disrupts Synaptic Plasticity by Altering Glutamate Recycling at the Synapse. J Alzheimers Dis (2014).
[43] Russell CL, Semerdjieva S, Empson RM, Austen BM, Beesley PW, Alifragis P. Amyloid-beta acts as a regulator of neurotransmitter release disrupting the interaction between synaptophysin and VAMP2. PLoS One 7(8): e43201 (2012).
[44] Lau CF, Ho YS, Hung CH, Wuwongse S, Poon CH, Chiu K, *et al.* Protective effects of testosterone on presynaptic terminals against oligomeric beta-amyloid peptide in primary culture of hippocampal neurons. Biomed Res Int 2014: 103906 (2014).
[45] Kelly BL, Ferreira A. Beta-amyloid disrupted synaptic vesicle endocytosis in cultured hippocampal neurons. Neuroscience 147(1): 60-70 (2007).
[46] Bell KF, Bennett DA, Cuello AC. Paradoxical upregulation of glutamatergic presynaptic boutons during mild cognitive impairment. J Neurosci 27(40): 10810-7 (2007).
[47] Sperling R. Functional MRI studies of associative encoding in normal aging, mild cognitive impairment, and Alzheimer's disease. Ann N Y Acad Sci 1097: 146-55 (2007).
[48] Hojo Y, Murakami G, Mukai H, Higo S, Hatanaka Y, Ogiue-Ikeda M, *et al.* Estrogen synthesis in the brain--role in synaptic plasticity and memory. Mol Cell Endocrinol 290(1-2): 31-43 (2008).
[49] Milner TA, Ayoola K, Drake CT, Herrick SP, Tabori NE, McEwen BS, *et al.* Ultrastructural localization of estrogen receptor beta immunoreactivity in the rat hippocampal formation. J Comp Neurol 491(2): 81-95 (2005).
[50] Milner TA, McEwen BS, Hayashi S, Li CJ, Reagan LP, Alves SE. Ultrastructural evidence that hippocampal alpha estrogen receptors are located at extranuclear sites. J Comp Neurol 429(3): 355-71 (2001).
[51] Ishunina TA, Swaab DF. Increased expression of estrogen receptor alpha and beta in the nucleus basalis of Meynert in Alzheimer's disease. Neurobiol Aging 22(3): 417-26 (2001).
[52] Ishunina TA, Swaab DF. Increased neuronal metabolic activity and estrogen receptors in the vertical limb of the diagonal band of Broca in Alzheimer's disease: relation to sex and aging. Exp Neurol 183(1): 159-72 (2003).
[53] Lu YP, Zeng M, Hu XY, Xu H, Swaab DF, Ravid R, *et al.* Estrogen receptor alpha-immunoreactive astrocytes are increased in the hippocampus in Alzheimer's disease. Exp Neurol 183(2): 482-8 (2003).
[54] Fitzpatrick JL, Mize AL, Wade CB, Harris JA, Shapiro RA, Dorsa DM. Estrogen-mediated neuroprotection against beta-amyloid toxicity requires expression of estrogen receptor alpha or beta and activation of the MAPK pathway. J Neurochem 82(3): 674-82 (2002).
[55] Cordey M, Pike CJ. Neuroprotective properties of selective estrogen receptor agonists in cultured neurons. Brain Res 1045(1-2): 217-23 (2005).
[56] Mateos L, Persson T, Katoozi S, Gil-Bea FJ, Cedazo-Minguez A. Estrogen protects against amyloid-beta toxicity by estrogen receptor alpha-mediated inhibition of Daxx translocation. Neurosci Lett 506(2): 245-50 (2012).
[57] Carbonaro V, Caraci F, Giuffrida ML, Merlo S, Canonico PL, Drago F, *et al.* Enhanced expression of ERalpha in astrocytes modifies the response of cortical neurons to beta-amyloid toxicity. Neurobiol Dis 33(3): 415-21 (2009).
[58] Zhao L, Brinton RD. Estrogen receptor alpha and beta differentially regulate intracellular Ca(2+) dynamics leading to ERK phosphorylation and estrogen neuroprotection in hippocampal neurons. Brain Res 1172: 48-59 (2007).
[59] Hwang CJ, Yun HM, Park KR, Song JK, Seo HO, Hyun BK, *et al.* Memory Impairment in Estrogen Receptor alpha Knockout Mice Through Accumulation of Amyloid-beta Peptides. Mol Neurobiol (2014).
[60] Merlo S, Sortino MA. Estrogen activates matrix metalloproteinases-2 and -9 to increase beta amyloid degradation. Mol Cell Neurosci 49(4): 423-9 (2012).
[61] Nord LC, Sundqvist J, Andersson E, Fried G. Analysis of oestrogen regulation of alpha-, beta- and gamma-secretase gene and protein expression in cultured human neuronal and glial cells. Neurodegener Dis 7(6): 349-64 (2010).
[62] Marin R, Ramirez CM, Gonzalez M, Gonzalez-Munoz E, Zorzano A, Camps M, *et al.* Voltage-dependent anion channel (VDAC) participates in amyloid beta-induced toxicity and interacts with plasma membrane estrogen receptor alpha in septal and hippocampal neurons. Mol Membr Biol 24(2): 148-60 (2007).
[63] Chen WF, Zhou LP, Chen L, Wu L, Gao QG, Wong MS. Involvement of IGF-I receptor and estrogen receptor pathways in the pro-

tective effects of ginsenoside Rg1 against Abeta(2)(5)(-)(3)(5)-induced toxicity in PC12 cells. Neurochem Int 62(8): 1065-71 (2013).

[64] Ong WY, Tanaka K, Dawe GS, Ittner LM, Farooqui AA. Slow excitotoxicity in Alzheimer's disease. J Alzheimers Dis 35(4): 643-68 (2013).

[65] Mizuno T. The biphasic role of microglia in Alzheimer's disease. Int J Alzheimers Dis 2012: 737846 (2012).

[66] Sortino MA, Chisari M, Merlo S, Vancheri C, Caruso M, Nicoletti F*, et al.* Glia mediates the neuroprotective action of estradiol on beta-amyloid-induced neuronal death. Endocrinology 145(11): 5080-6 (2004).

Received: ???????????????? **Revised:** ???????????????? **Accepted:** ????????????????